MCB
Journals.ASM.org

BRG1 Is Required for Formation of Senescence-Associated Heterochromatin Foci Induced by Oncogenic RAS or BRCA1 Loss

Zhigang Tu,[a] Xinying Zhuang,[b] Yong-Gang Yao,[b] Rugang Zhang[a]

Gene Expression and Regulation Program, The Wistar Institute, Philadelphia, Pennsylvania, USA[a]; Key Laboratory of Animal Models and Human Disease Mechanisms of the Chinese Academy of Sciences, Kunming Institute of Zoology, Kunming, Yunnan, China[b]

Cellular senescence is an important tumor suppression mechanism. We have previously reported that both oncogene-induced dissociation of BRCA1 from chromatin and BRCA1 knockdown itself drive senescence by promoting formation of senescence-associated heterochromatin foci (SAHF). However, the molecular mechanism by which BRCA1 regulates SAHF formation and senescence is unclear. BRG1 is a chromatin-remodeling factor that interacts with BRCA1 and pRB. Here we show that BRG1 is required for SAHF formation and senescence induced by oncogenic RAS or BRCA1 loss. The interaction between BRG1 and BRCA1 is disrupted during senescence. This correlates with an increased level of chromatin-associated BRG1 in senescent cells. BRG1 knockdown suppresses the formation of SAHF and senescence, while it has no effect on BRCA1 chromatin dissociation induced by oncogenic RAS, indicating that BRG1 functions downstream of BRCA1 chromatin dissociation. Furthermore, BRG1 knockdown inhibits SAHF formation and senescence induced by BRCA1 knockdown. Conversely, BRG1 overexpression drives SAHF formation and senescence in a DNA damage-independent manner. This effect depends upon BRG1's chromatin-remodeling activity as well as the interaction between BRG1 and pRB. Indeed, the interaction between BRG1 and pRB is enhanced during senescence. Chromatin immunoprecipitation analysis revealed that BRG1's association with the human *CDKN2A* and *CDKN1A* gene promoters was enhanced during senescence induced by oncogenic RAS or BRCA1 knockdown. Consistently, knockdown of pRB, $p21^{CIP1}$, and $p16^{INK4a}$, but not p53, suppressed SAHF formation induced by BRG1. Together, these studies reveal the molecular underpinning by which BRG1 acts downstream of BRCA1 to promote SAHF formation and senescence.

Activation of oncogenes (such as RAS) in primary mammalian cells typically triggers cellular senescence, a state of irreversible cell growth arrest (1, 2). Oncogene-induced senescence is an important tumor suppression mechanism *in vivo* (1). Senescent cells display several morphological and molecular characteristics. For instance, they are positive for senescence-associated β-galactosidase (SA-β-gal) activity (3). In addition, chromatin in the nuclei of senescent human cells typically reorganizes to form specialized domains of facultative heterochromatin called senescence-associated heterochromatin foci (SAHF) (4–8). SAHF are enriched in markers of heterochromatin such as histone H2A variant macroH2A (mH2A), di- or trimethylated lysine 9 histone H3 (H3K9Me2/3), and heterochromatin protein 1 (HP1) proteins (5, 7). SAHF formation contributes to the senescence-associated cell cycle exit by directly sequestering and silencing proliferation-promoting genes (4, 7). The p53 and pRB tumor suppressor pathways are the key regulators of senescence (1). Indeed, $p16^{INK4a}$, an upstream regulator of pRB, and $p21^{CIP1}$, a downstream target of p53, promote SAHF formation (7, 9). In addition, senescence induced by oncogenic RAS is characterized by a DNA damage response (10) and is accompanied by the accumulation of markers of DNA damage such as upregulation of γH2AX protein expression and increased formation of γH2AX DNA damage foci (10, 11).

BRCA1 plays an important role in DNA damage repair (12, 13). Germ line mutations in the *BRCA1* gene predispose women to breast and ovarian cancer (12). We have previously demonstrated that BRCA1 becomes dissociated from chromatin in response to activation of oncogenes such as RAS (14). This promotes senescence by driving SAHF formation (14). In addition, BRCA1 chromatin dissociation contributes to the accumulation of DNA damage by impairing the BRCA1-mediated DNA repair response (14). Similarly, we showed that BRCA1 knockdown drives SAHF formation and senescence and triggers the DNA damage response (14). It has also been shown that cells from the *BRCA1* exon 11 knockout mouse exhibit signs of premature senescence (15, 16). However, the molecular mechanism by which BRCA1 regulates SAHF formation and senescence remains to be determined. In addition, it is unclear whether SAHF formation induced by BRCA1 chromatin dissociation or BRCA1 knockdown is independent of the DNA damage response.

BRCA1 has also been implicated in regulating high-order chromatin structure. For example, targeting BRCA1 to an amplified *lac* operator-containing chromosome region in the mammalian genome results in large-scale chromatin unfolding (17). This suggests that BRCA1 antagonizes heterochromatin formation. Notably, BRCA1 also interacts with the BRG1 subunit of the ATP-dependent SWI/SNF chromatin-remodeling complex (18). BRG1 acts as an activator or repressor of gene expression in a context-dependent manner (19). Loss of BRG1 function is associated with malignant transformation (19), and BRG1 heterozygous deletion results in spontaneous tumor development in mouse models, indicating its role as a tumor suppressor (20, 21). Notably, BRG1 interacts with pRB (22), a key regulator of SAHF formation and

Received 27 December 2012 Returned for modification 19 January 2013
Accepted 19 February 2013
Published ahead of print 25 February 2013
Address correspondence to Rugang Zhang, rzhang@wistar.org.
Supplemental material for this article may be found at http://dx.doi.org/10.1128/MCB.01744-12.

doi:10.1128/MCB.01744-12

senescence (4, 7, 23). BRG1 also plays a role in promoting cell growth arrest and senescence phenotypes (22, 24–27). However, whether the interaction between BRG1 and BRCA1 or pRB is regulated during senescence is unknown. In addition, whether BRG1 contributes to SAHF formation induced by oncogenic RAS or BRCA1 knockdown has never been investigated.

Here we show that the interaction between BRCA1 and BRG1 is disrupted in cells undergoing senescence. This correlates with an increased level of chromatin-associated BRG1 in senescent cells. BRG1 is required for SAHF formation and senescence induced by BRCA1 chromatin dissociation or BRCA1 knockdown. Conversely, ectopic BRG1 drives SAHF formation and senescence, which requires its chromatin-remodeling activity to upregulate $p16^{INK4a}$ and $p21^{CIP1}$. Indeed, the association of BRG1 with the promoters of the SAHF-regulating genes *CDKN2A* (encoding $p16^{INK4a}$) and *CDKN1A* (encoding $p21^{CIP1}$) was enhanced during senescence induced by oncogene activation or BRCA1 knockdown. Interestingly, BRG1 promotes SAHF and senescence in a DNA damage response-independent manner. Further, we show that the interaction between BRG1 and pRB is enhanced during senescence and that SAHF formation induced by ectopic BRG1 requires its interaction with pRB. Finally, we found that knockdown of pRB, $p16^{INK4a}$, and $p21^{CIP1}$, but not p53, impairs SAHF formation induced by BRG1.

MATERIALS AND METHODS

Cell culture. IMR90 cells were cultured according to the ATCC and as previously described (5, 23). Experiments were performed on IMR90 cells between population doublings 25 and 35.

Plasmids, antibodies, and immunoblotting. pBABE-puro, pBABE-puro-H-RAS^{G12V}, pBABE-puro-BRG1, and pBABE-puro-BRG1 (K798R) were obtained from Addgene. The BRCA1 short hairpin RNAs (shRNAs) were described previously (14). pBABE-puro-BRG1 delRB with a deletion of amino acids (aa) 1357 to 1361 (BRG1 ΔRB) was generated using standard molecular cloning techniques. Lentivirus-encoded shRNAs were purchased from Open Biosystems. The sense strand sequences for the BRG1 shRNAs are 5′-CCCGTGGACTTCAAGAAGATA-3′ and 5′-CGGCAGACACTGTGATCATTT-3′. The sense strand sequences for the $p16^{INK4a}$ shRNAs are 5′-CATGGAGCCTTCGGCTGACT-3′ and 5′-GCGCTGCCCAACGCACCGAAT-3′. The sense strand sequences for the $p21^{CIP1}$ shRNAs are 5′-CGCTCTACATCTTCTGCCTTA-3′ and 5′-GACAGATTTCTACCACTCCAA-3′. The sense strand sequences for the pRB shRNAs are 5′-CCACATTATTTCTAGTCCAAA-3′ and 5′-CAGAGATCGTGTATTGAGATT-3′. The sense strand sequences for the p53 shRNAs are 5′-GAGGGATGTTTGGGAGATGTA-3′ and 5′-GTCCAGATGAAGCTCCCAGAA-3′. The following antibodies were obtained from the indicated suppliers: rabbit anti-BRCA1 (Upstate), mouse anti-BRCA1 (Calbiochem) (for immunofluorescence staining), rabbit anti-BRG1 (Santa Cruz), mouse anti-$p21^{CIP1}$ (Santa Cruz), mouse anti-$p16^{INK4a}$ (Santa Cruz), mouse anti-β-actin (Sigma), mouse anti-RAS (BD Bioscience), mouse anti-p53 (Calbiochem), rabbit anti-serine 15-phosphorylated p53 (Cell Signaling), rabbit anti-FLAG (Cell Signaling), mouse anti-pRB (Cell Signaling), rabbit anti-histone H3 (Millipore), and mouse anti-H3K9me2 (Abcam). Rabbit anti-mH2A1.2 was described previously (4, 28). Immunoblotting was performed using standard protocols with the antibodies indicated above.

Retrovirus and lentivirus infections. Retrovirus production and transduction were performed as described previously (5, 29) using Phoenix cells to package the infection viruses (Gary Nolan, Stanford University). Lentivirus was packaged using a Virapower kit from Invitrogen by following the manufacturer's instructions and as described previously (29, 30). Cells infected with viruses carrying a gene conferring resistance to puromycin or neomycin were selected in 1 μg/ml puromycin or 500 μg/ml neomycin (G418), respectively.

Co-IP analysis. Cells were washed twice with phosphate-buffered saline (PBS) and lysed using a buffer containing 50 mM Tris-HCl (pH 8.0), 1 mM EDTA, 0.5% NP-40, and 150 mM NaCl with the proteinase inhibitors. The supernatant was collected by centrifuging the cell lysates at 12,000 × *g* for 10 min at 4°C. One milligram of total protein supernatant was subjected to immunoprecipitation (IP) using 2 μg anti-FLAG antibody (Sigma), anti-BRG1 antibody (Santa Cruz), or an isotype-matched IgG control by incubating the antibodies with supernatant for 2 h at 4°C. The IP products were separated on an SDS-PAGE gel and immunoblotted with anti-pRB, anti-BRCA1, or anti-BRG1 antibodies to visualize the immunoprecipitated proteins.

Chromatin isolation and chromatin immunoprecipitation (ChIP) analysis. Chromatin was prepared according to previously published methods (6, 31). Chromatin-bound proteins in the chromatin fraction were detected by immunoblotting using antibodies against BRCA1, BRG1, and histone H3 as indicated above.

ChIP analysis in control, RAS-infected, or BRCA1 knockdown IMR90 cells was performed at day 4 post-drug selection as previously described (14) using a polyclonal anti-BRG1 antibody (Santa Cruz), an anti-BRCA1 antibody (Millipore), or an isotype-matched IgG control. Immunoprecipitated DNA was analyzed by PCR or SYBR green-based quantitative PCR (Qiagen). Primers against the human *CDKN2A* gene promoter region are 5′-TGATTTCGATTCTCGGTGGG-3′ and 5′-GGGTGTTTGGTGTCATAGGG-3′. Primers against the human *CDKN1A* gene promoter region are 5′-TTCAGGAGACAGACAACTCACTC-3′ and 5′-GACACCCCAACAAAGCATCTTG-3′.

Immunofluorescence and SA-β-gal staining. Immunofluorescence staining was performed as described previously using the antibodies described above (4, 5, 28). SA-β-gal staining was performed as previously described (3).

Comet assay. A comet assay was performed with a CometAssay (Trevigen) kit following the manufacturer's instruction. DNA damage was measured in artificial Olive Moment units using Cometscore software. A *t* test for significance was performed using Graph Prism software.

RESULTS

The interaction between BRCA1 and BRG1 is disrupted in cells undergoing senescence, which correlates with an increased level of chromatin-associated BRG1 and an enhanced interaction between BRG1 and pRB. We have previously shown that oncogenic RAS dissociates BRCA1 from chromatin, which contributes to formation of SAHF and the senescence phenotype (14). Notably, BRCA1 chromatin dissociation is not a consequence of G_1 phase accumulation in the fully established senescence cells (14), because BRCA1 becomes dissociated from chromatin prior to G_1 phase accumulation in RAS-infected cells compared with controls (see Fig. S1 in the supplemental material). Likewise, knockdown of BRCA1 in primary human cells induces formation of SAHF and senescence (14). Given the role of $p16^{INK4a}$ and $p21^{CIP1}$ in promoting SAHF formation and senescence (2), we first examined changes in the expression of $p16^{INK4a}$ and $p21^{CIP1}$ in IMR90 normal human fibroblasts expressing shRNAs corresponding to the human *BRCA1* gene (shBRCA1) that efficiently knock down BRCA1 protein expression (Fig. 1A). Compared with controls, the expression of both $p16^{INK4a}$ and $p21^{CIP1}$ was upregulated in BRCA1 knockdown cells (Fig. 1B). Notably, similar results were obtained by multiple shBRCA1s (Fig. 1A and B), suggesting that the observed phenotype was not due to off-target effects.

It has been demonstrated that BRCA1 interacts with BRG1, an ATP-dependent chromatin-remodeling factor, in transformed cancer cells (18). In addition, the *CDKN2A* and *CDKN1A* genes,

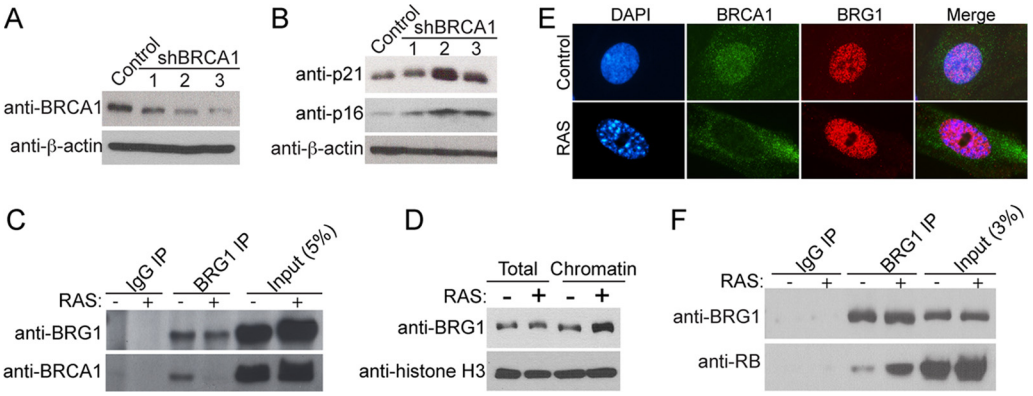

FIG 1 The interaction between BRG1 and BRCA1 is disrupted during senescence, which correlates with an increased level of chromatin-associated BRG1. (A) IMR90 normal human fibroblasts were infected with lentivirus encoding the indicated shBRCA1 or the control. Drug-selected cells were examined for the expression of BRCA1 and β-actin by immunoblotting. (B) Same as described for panel A except that cells were examined for the expression of $p21^{CIP1}$ and $p16^{INK4a}$ by immunoblotting. (C) IMR90 cells were infected with retrovirus encoding control or oncogenic $H\text{-}RAS^{G12V}$. Drug-selected cells were subjected to coimmunoprecipitation experiments using an anti-BRG1 antibody. An isotype-matched IgG was used as a negative control. Levels of immunoprecipitated BRG1 and BRCA1 were determined by immunoblotting using the indicated antibodies. (D) Same as described for panel C except that the cells were subjected to fractionation to prepare chromatin and the expression of BRG1 and histone H3 in the chromatin fraction of the indicated cells was examined by immunoblotting. (E) Same as described for panel C except that the cells were subjected to immunofluorescence staining using anti-BRCA1 and anti-BRG1 antibodies. DAPI, 4′,6′diamidino-2-phenylindole. (F) Same as described for panel C except that the cells were subjected to coimmunoprecipitation experiments using an anti-BRG1 antibody. An isotype-matched IgG was used as a negative control. Levels of immunoprecipitated BRG1 and pRB were determined by immunoblotting using the indicated antibodies.

which respectively encode $p16^{INK4a}$ and $p21^{CIP1}$ proteins, are known BRG1 target genes (24, 32). Thus, we sought to determine whether the interaction between BRCA1 and BRG1 is regulated during senescence of IMR90 fibroblasts induced by oncogenic RAS. Toward this goal, IMR90 cells expressing oncogenic RAS to induce senescence or control were subjected to co-immunoprecipitation (co-IP) using an anti-BRG1 antibody. An isotype-matched IgG was used a negative control. Consistent with the previous observations in cancer cells (18), we found that BRG1 is associated with BRCA1 in control proliferating cells by co-IP analysis (Fig. 1C). Interestingly, we found that this association was lost in RAS-infected cells (Fig. 1C). This was not due to a decrease of either BRCA1 or BRG1 expression level, as the input levels of BRCA1 and BRG1 are comparable between control and RAS-infected cells at this time point (Fig. 1C). Notably, the co-IP demonstrated a high stoichiometry of BRG1 and BRCA1 complex formation, as pulling down BRG1 brought down a similar fraction of BRCA1 (Fig. 1C). Since BRCA1 became dissociated from chromatin (14) and the interaction between BRG1 and BRCA1 was disrupted during senescence (Fig. 1C), we examined the changes in the levels of BRG1 in chromatin fractions during senescence. In contrast to BRCA1's chromatin dissociation (14), BRG1 levels in the chromatin fraction were increased in RAS-infected cells compared with controls (Fig. 1D). This was not due to an increase in total BRG1 levels in RAS-infected cells compared to controls (Fig. 1D). Consistently, immunofluorescence staining of BRCA1 and BRG1 showed that the colocalization between BRCA1 and BRG1 was decreased in the nuclei of RAS-induced senescent cells compared with controls (Fig. 1E). Based on this result, we conclude that the interaction between BRCA1 and BRG1 is disrupted and chromatin-associated BRG1 levels are increased in cells undergoing senescence.

BRG1 interacts with pRB, a known regulator of SAHF formation and senescence (7, 22, 23). Thus, we sought to determine whether the interaction between BRG1 and pRB is regulated during senescence. To do so, we performed co-IP using an anti-BRG1 antibody in control and RAS-infected cells. An isotype-matched IgG was used as a control. Interestingly, the interaction between BRG1 and pRB was enhanced in cells undergoing senescence (Fig. 1F).

Ectopic BRG1 drives SAHF formation and senescence. Knockout of BRG1 results in the dissolution of pericentromeric heterochromatin (33), suggesting that BRG1 plays a role in regulating heterochromatin structure. Therefore, we next sought to determine whether ectopic BRG1 is sufficient to drive SAHF formation. Toward this goal, we ectopically expressed wild-type BRG1 in IMR90 normal human fibroblasts (Fig. 2A). Indeed, there was a significant increase in SAHF formation in cells ectopically expressing BRG1 compared with controls (Fig. 2B and C). Consistently, other markers of SAHF such as formation of H3K9Me2 and mH2A1.2 foci were also induced by the ectopically expressed wild-type BRG1 (Fig. 2B and C). Expression of SA-β-gal activity, a hallmark of cellular senescence (3), was also induced by wild-type BRG1 expression (Fig. 2D and E). Thus, we conclude that ectopic expression of wild-type BRG1 drives SAHF formation and senescence.

We next sought to determine whether BRG1's ability to drive SAHF formation is dependent upon its chromatin-remodeling activity. To do so, we obtained a mutant BRG1 with a single amino acid substitution at amino acid residue 798 (BRG1 K798R), which has previously been demonstrated to be deficient in chromatin-remodeling activity (34). Compared with wild-type controls, the mutant BRG1 that is deficient in chromatin-remodeling activity was also severely impaired in its ability to drive SAHF formation and the expression of SA-β-gal activity (Fig. 2A to E). Since $p16^{INK4a}$ and $p21^{CIP1}$ are key regulators of SAHF formation and are known BRG1 target genes (7, 9, 24, 32), we next examined the expression of $p16^{INK4a}$ and $p21^{CIP1}$ in cells expressing the control, wild-type BRG1, and the mutant BRG1. Compared with controls, the expression of both $p16^{INK4a}$ and $p21^{CIP1}$ was upregulated by

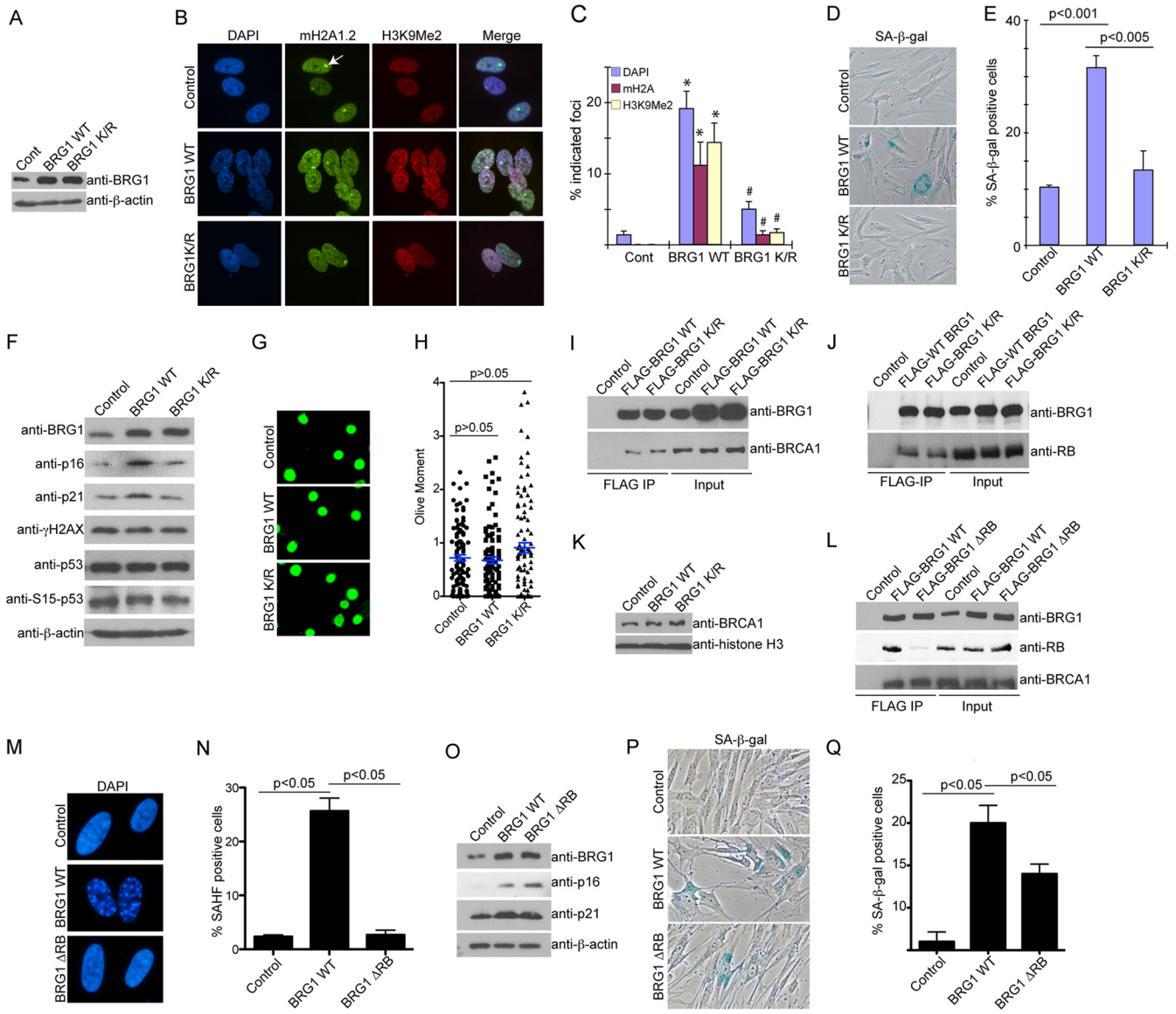

FIG 2 Ectopic expression of BRG1 drives SAHF formation and senescence, which is dependent upon its chromatin-remodeling activity. (A) IMR90 cells were infected with retrovirus encoding a wild-type BRG (BRG WT), a K798R mutant BRG1 that is defective in chromatin-remodeling activity (BRG1 K/R), or the control (Cont). Expression of BRG1 was examined by immunoblotting in the drug-selected cells. Expression of β-actin was used as a loading control. (B) Same as described for panel A except that cells were stained with DAPI and the indicated antibodies to visualize SAHF. The arrow points to an example of inactivated X chromosome stained by mH2A1.2 antibody in control IMR90 cells. (C) Quantitation of the results shown in panel B. A total of 200 cells from each of the indicated groups were examined for the expression of the indicated markers. Data represent the means of the results of three independent experiments with standard deviations (SD). *, $P < 0.05$ (compared with controls); #, $P < 0.05$ (compared with wild-type BRG1). (D) Same as described for panel A except that cells were stained for SA-β-gal activity. (E) Quantitation of the results shown in panel D. A total of 200 cells from each of the indicated groups were examined for expression of SA-β-gal activity. Data represent the means of the results of three independent experiments with SD. (F) Same as described for panel A except that cells were examined for expression of BRG1, $p16^{INK4a}$, $p21^{CIP1}$, p53, serine 15-phosphorylated p53 (S15-p53), and γH2AX by immunoblotting. Expression of β-actin was used as a loading control. (G) Same as described for panel A except that cells were measured for the extent of DNA damage using the comet assay. Note that these experiments were performed at the same time as those shown in Fig. 4I, where shBRCA1-expressing cells were used as positive controls. (H) Quantification of the results shown in panel G. The extent of DNA damage measured by the comet assay was calculated as artificial Olive Moment units as described in Materials and Methods. Olive Moment levels in 100 cells from each group were measured. Means of the data representing Olive Moment units with standard errors of the means (SEM) are shown in blue. (I) IMR90 cells were infected with retrovirus encoding FLAG-tagged wild-type BRG1, the BRG1 K/R mutant, or the control. Drug-selected cells were subjected to coimmunoprecipitation experiments using an anti-FLAG antibody. An isotype-matched IgG was used as a negative control. Levels of immunoprecipitated BRG1 and BRCA1 were determined by immunoblotting using the indicated antibodies. (J) Same as described for panel I except that cells were examined for the levels of immunoprecipitated BRG1 and pRB. (K) Same as described for panel A except that cells were subjected to fractionation to prepare chromatin and the expression of BRCA1 and histone H3 in the chromatin fraction of the indicated cells was examined by immunoblotting. (L) IMR90 cells were infected with retrovirus encoding FLAG-tagged wild-type BRG1 (BRG1 WT), BRG1 with aa 1357 to 1361 deleted (BRG1 ΔRB), or the control. Drug-selected cells were subjected to coimmunoprecipitation experiments using an anti-FLAG antibody. An isotype-matched IgG was used as a negative control. Levels of immunoprecipitated BRG1, pRB, and BRCA1 were determined by immunoblotting using the indicated antibodies. (M) Same as described for panel L except that cells were stained with DAPI to visualize SAHF formation. (N) Quantification of the results shown in panel M. A total of 200 cells from each of the indicated groups were examined for SAHF formation. Data represent the means of the results of three independent experiments with SD. (O) Same as described for panel L except that cells were examined for BRG1, $p21^{CIP1}$, $p16^{INK4a}$, and β-actin expression by immunoblotting using the indicated antibodies. (P) Same as described for panel L except that cells were stained for SA-β-gal activity. (Q) Quantification of the results shown in panel P. A total of 200 cells from each of the indicated groups were examined for SA-β-gal activity. Data represent the means of the results of three independent experiments with SD.

wild-type BRG1 but not mutant BRG1 that is deficient in chromatin-remodeling activity (Fig. 2F). Together, we conclude that the chromatin-remodeling activity of BRG1 is required for SAHF formation and senescence, which correlates with the upregulation of $p16^{INK4a}$ and $p21^{CIP1}$ in these cells.

Since formation of SAHF and senescence induced by BRCA1 knockdown or oncogenic RAS is accompanied by the accumulation of DNA damage (see Fig. S1C in the supplemental material) (14), we next examined the expression of γH2AX, a marker of DNA damage, in cells expressing wild-type BRG1 or mutant BRG1 (BRG1 K798R). Interestingly, the expression of γH2AX was not upregulated by the expression of wild-type or mutant BRG1 compared with controls (Fig. 2F). Likewise, the formation of γH2AX foci was not significantly induced by wild-type BRG1 (see Fig. S2 in the supplemental material). Further, the expression of p53 or serine 15 phosphorylated p53 was not upregulated by the expression of either wild-type or mutant BRG1 (Fig. 2F). We next directly measured the extent of DNA damage in these cells using the comet assay. Compared with controls, the extent of DNA damage was not significantly affected by either wild-type or mutant BRG1 (Fig. 2G and H). Interestingly, both wild-type BRG1 and the BRG1 K798R mutant were able to interact with BRCA1 (Fig. 2I), suggesting that the inability of the BRG1 K798R mutant to induce SAHF formation and senescence was not due to an impaired interaction with BRCA1. In addition, the interaction between BRG1 and pRB was not disrupted by the BRG1 K798R mutant, suggesting that the observed effects were not due to a complete misfolding of the mutant protein (Fig. 2J). Notably, ectopically expressed BRG1 did not dissociate BRCA1 from chromatin (Fig. 2K), suggesting that BRG1 acts downstream of BRCA1 chromatin dissociation. We previously showed that oncogene-induced BRCA1 chromatin dissociation contributes to both SAHF formation and DNA damage accumulation (14). Likewise, BRCA1 knockdown triggers SAHF formation and DNA damage response (14). Here we showed that ectopic BRG1 drove SAHF formation but not the DNA damage response and that BRG1 did not dissociate BRCA1 from chromatin (Fig. 2B, C, F to H, and K). Together, these data support the premise that BRG1 acts downstream of BRCA1 chromatin dissociation to promote SAHF formation during senescence.

Next, we sought to determine the importance of the interaction between BRG1 and pRB in formation of SAHF induced by BRG1. Toward this goal, we generated a mutant BRG1 that no longer binds to pRB (deletion of aa 1357 to 1361; BRG1 ΔRB) (22, 35, 36) and confirmed the disruption of the interaction between BRG1 ΔRB and pRB by co-IP analysis (Fig. 2L). Notably, the BRG1 ΔRB mutant retained its ability to interact with BRCA1 (Fig. 2L). This result suggests that the effects observed in the BRG1 ΔRB mutant were not due to a complete misfolding of the protein. Indeed, compared with wild-type BRG1, the BRG1 ΔRB mutant was significantly impaired in its ability to drive SAHF formation (Fig. 2M and N). Interestingly, compared with wild-type BRG1, there was no overt difference in induction of $p16^{INK4a}$ and $p21^{CIP1}$ by the BRG1 ΔRB mutant (Fig. 2O). Given that the BRG1 chromatin-remodeling-activity-deficient mutant (BRG1 K798R) failed to upregulate $p16^{INK4a}$ and $p21^{CIP1}$ (Fig. 2F), this result suggests that upregulation of $p16^{INK4a}$ and $p21^{CIP1}$ expression induced by BRG1 functions upstream of pRB, which is independent of the interaction between BRG1 and pRB and dependent on BRG1's chromatin-remodeling activity. Consistently, compared with wild-type BRG1, levels of other markers of senescence such as SA-β-gal activity were decreased in BRG1 ΔRB mutant-expressing cells, albeit to a much lesser extent than that seen SAHF formation in wild-type BRG1-expressing cells (Fig. 2P and Q). Based on these results, we conclude that the interaction between BRG1 and pRB is enhanced in cells undergoing senescence and that SAHF formation induced by BRG1 requires its interaction with pRB.

Knockdown of BRG1 suppresses SAHF formation and senescence induced by oncogenic RAS. We next sought to determine whether BRG1 is required for the SAHF formation and senescence that is associated with BRCA1 chromatin dissociation induced by oncogenic RAS. To do so, we obtained two individual shRNAs corresponding to the human *BRG1* gene (shBRG1) that can efficiently knock down BRG1 expression (e.g., see Fig. 3D). We infected IMR90 cells with oncogenic RAS to induce BRCA1 chromatin dissociation, SAHF formation, and senescence together with shBRG1 or the control. Compared with RAS-alone cells, knockdown of BRG1 significantly suppressed the RAS-induced SA-β-gal activity and SAHF formation (Fig. 3A to C). However, BRG1 knockdown itself had no effects on expression of markers of senescence such as SA-β-gal activity or SAHF formation (see Fig. S3 in the supplemental material). Interestingly, BRG1 knockdown in mesenchymal stem cells induces the senescence phenotype (27). The discrepancy may be explained by differences in the experimental systems. Notably, the expression of both $p16^{INK4a}$ and $p21^{CIP1}$ was significantly downregulated by shBRG1 compared with RAS-alone controls (Fig. 3D). This was not due to a lower level of RAS expression in BRG1 knockdown cells, as the RAS expression was comparable (Fig. 3D). Interestingly, BRG1 knockdown had no effects on BRCA1 chromatin dissociation induced by oncogenic RAS (Fig. 3E). This result further supports the premise that BRG1 functions downstream of RAS-induced BRCA1 chromatin dissociation. Consistently, BRG1 knockdown did not overtly affect RAS-induced DNA damage accumulation. For example, RAS-induced upregulation of γH2AX expression or formation of γH2AX foci was not significantly affected by shBRG1 compared with controls (Fig. 3F; see also Fig. S4 in the supplemental material). Based on these results, we conclude that knockdown of BRG1 suppresses RAS-induced SAHF formation and senescence, which is independent of the DNA damage response.

Our results suggest that BRG1 contributes to SAHF formation and senescence induced by oncogenic RAS by promoting $p16^{INK4a}$ and $p21^{CIP1}$ expression, which depends upon BRG1's chromatin-remodeling activity (Fig. 2). Thus, we examined the association of BRG1 with the promoters of the *CDKN2A* (encoding $p16^{INK4a}$) and *CDKN1A* (encoding $p21^{CIP1}$) genes in IMR90 cells infected with oncogenic RAS by ChIP using an anti-BRG1 antibody. An isotype-matched IgG was used a negative control for ChIP analysis. Compared with controls, BRG1's association with the promoters of both *CDKN2A* and *CDKN1A* genes was significantly enhanced in RAS-infected cells (Fig. 3G to J). In contrast, compared with controls, there was no overt change in BRCA1's association with the promoters of either the *CDKN2A* or *CDKN1A* gene in RAS-infected cells (see Fig. S5 in the supplemental material).

BRG1 enhances senescence induced by BRCA1 knockdown, and knockdown of BRG1 suppresses SAHF formation and senescence induced by BRCA1 knockdown. We next sought to determine whether ectopic expression of BRG1 enhances the senescence phenotype induced by BRCA1 knockdown. Toward this

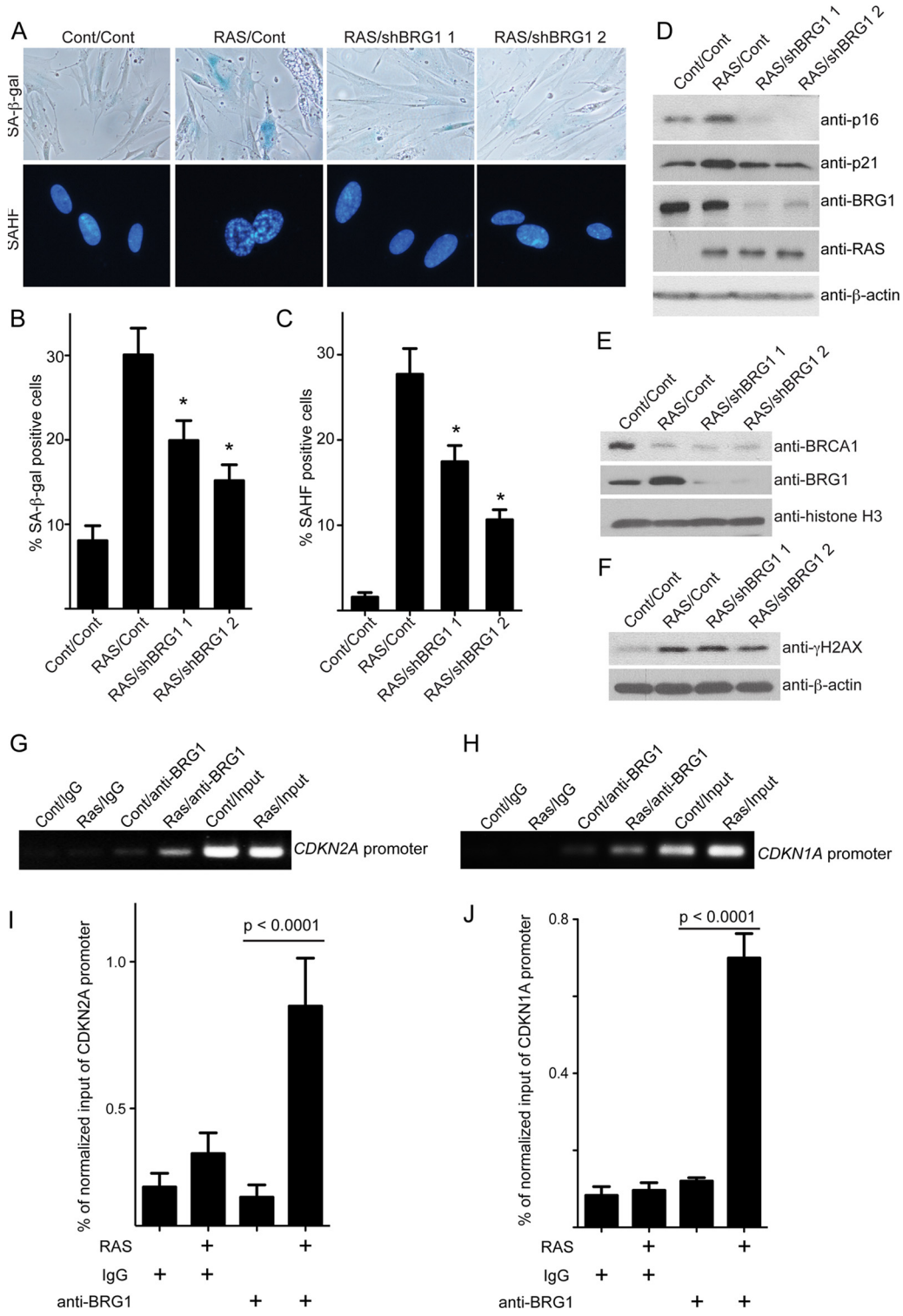

FIG 3 Knockdown of BRG1 suppresses SAHF formation and senescence induced by oncogenic RAS. (A) IMR90 cells were infected with retrovirus encoding oncogenic H-RAS^{G12V} together with lentivirus encoding the indicated shBRG1 or the control. Drug-selected cells were stained for SA-β-gal activity or DAPI to visualize SAHF formation. (B and C) Quantitation of the results shown in panel A. A total of 200 cells from each of the indicated group were examined for SA-β-gal activity or SAHF formation. Data represent the means of the results of three independent experiments with SD. *, $P < 0.05$ (compared with cells with RAS alone). (D) Same as described for panel A except that cells were examined for expression of p16^{INK4a}, p21^{CIP1}, BRG1, and RAS by immunoblotting. Expression of β-actin was used as a loading control. (E) Same as described for panel A except that the cells were subjected to fractionation to prepare chromatin and the expression of BRCA1 and BRG1 in the chromatin fraction of the indicated cells was examined by immunoblotting. Expression of histone H3 was used as a loading control. (F) Same as described for panel A except that cells were examined for expression of γH2AX by immunoblotting. Expression of β-actin was used as a loading control. (G) IMR90 cells were infected with retrovirus encoding oncogenic H-RAS^{G12V} or the control. Drug-selected cells were used to perform chromatin immunoprecipitation (ChIP) using an anti-BRG1 antibody. An isotype-matched IgG was used as a negative control for ChIP analysis. The immunoprecipitated DNA was subjected to PCR analysis using primers that amplify the promoter region of the human *CDKN2A* gene. (H) Same as described for panel G except that the immunoprecipitated DNA was subjected to quantitative PCR analysis. Data represent the means of the results of three independent experiments with SD. (I and J) Same as described for panels H and G except that the human *CDKN1A* gene promoter was analyzed.

goal, we infected IMR90 fibroblasts with a lentivirus encoding shBRCA1 together with a retrovirus encoding the wild type or the chromatin-remodeling-activity-deficient BRG1 mutant (BRG1 K798R). Compared with shBRCA1-alone cells, expression of wild-type BRG1 but not mutant BRG1 induced a more pronounced senescence phenotype, as indicated by a significant increase in SAHF formation and expression of SA-β-gal activity (Fig. 4A to C). Notably, this correlated with an increased induction of $p16^{INK4a}$ and $p21^{CIP1}$ but not γH2AX expression (Fig. 4D). Based on these results, we conclude that ectopic BRG1 enhances the senescence phenotype induced by BRCA1 knockdown, which correlates with enhanced expression of $p16^{INK4a}$ and $p21^{CIP1}$.

Our evidence supports the hypothesis that BRG1 acts downstream of BRCA1 chromatin dissociation to promote SAHF formation during RAS-induced senescence. We next wanted to directly test the effects of BRG1 knockdown on SAHF formation and senescence induced by BRCA1 knockdown. To do this, we infected IMR90 cells with a lentivirus encoding shBRCA1 together with a lentivirus encoding shBRG1 or the control. Compared with shBRCA1-alone cells, BRG1 knockdown significantly suppressed the expression of SA-β-gal activity and SAHF formation induced by BRCA1 knockdown (Fig. 4E to G). This was accompanied by a notable downregulation of $p16^{INK4a}$ and $p21^{CIP1}$ in shBRCA1/shBRG1-expressing cells compared with shBRCA1-alone cells (Fig. 4H). Taken together, these data indicate that BRG1 contributes to SAHF formation and senescence induced by BRCA knockdown and that this correlates with its effects on the expression of $p16^{INK4a}$ and $p21^{CIP1}$.

We next sought to determine the effects of BRG1 knockdown on the DNA damage induced by BRCA1 knockdown by examining γH2AX expression and directly measuring the extent of DNA damage in these cells using the comet assay. Notably, BRG1 knockdown did not overtly affect BRCA1 knockdown-induced γH2AX expression (Fig. 4H). Likewise, BRG1 knockdown did not significantly affect the extent of DNA damage induced by BRCA1 knockdown as measured by the comet assay (Fig. 4I and J). Taking these results together, we conclude that BRG1 knockdown does not suppress the DNA damage response induced by BRCA1 knockdown.

Notably, chromatin-associated BRG1 levels were increased in BRCA1 knockdown cells (Fig. 4K), further supporting the notion that BRCA1 functions upstream of BRG1. This was not due to an increase in the total BRG1 protein level in BRCA1 knockdown cells (Fig. 4K). Since BRCA1 knockdown induces the expression of $p21^{CIP1}$ and $p16^{INK4a}$, we next examined the association of BRG1 with the promoters of *CDKN2A* and *CDKN1A* genes in BRCA1 knockdown cells. Similar to what we observed in cells expressing oncogenic RAS, which induces dissociation of BRCA1 from chromatin, we observed that BRG1's association with the promoters of *CDKN2A* and *CDKN1A* genes was significantly enhanced in BRCA1 knockdown cells compared with controls (Fig. 4L to O). Together, these results further support the premise that BRG1 contributes to SAHF formation and senescence induced by BRCA1 chromatin dissociation or BRCA1 knockdown through promoting $p16^{INK4a}$ and $p21^{CIP1}$ expression.

Knockdown of pRB, $p16^{INK4a}$, and $p21^{CIP1}$, but not p53, inhibits SAHF formation induced by ectopic BRG1 expression. We showed that $p16^{INK4a}$ and $p21^{CIP1}$ expression is induced by BRG1 (Fig. 2F). In addition, a mutant BRG1 (BRG1 K798R) that is deficient in chromatin-remodeling activity is also impaired in SAHF formation (Fig. 2B and C). Further, we showed that the interaction between BRG1 and pRB is required for SAHF formation induced by BRG1 (Fig. 2M and N). However, we failed to observe an increase in p53 expression in BRG1-expressing cells (Fig. 2F). We next sought to directly determine the effects of knockdown of pRB, $p16^{INK4a}$, $p21^{CIP1}$, or p53 on SAHF formation induced by ectopic BRG1. To do so, we developed two individual shRNAs corresponding to the human *CDKN2A*, *CDKN1A*, *pRB*, or *p53* gene. The knockdown efficacy of these shRNAs was confirmed by immunoblotting using antibodies specific to pRB, $p16^{INK4a}$, $p21^{CIP1}$, and p53 (Fig. 5A to D). Interestingly, knockdown of pRB, $p16^{INK4a}$, or $p21^{CIP1}$ inhibited SAHF formation induced by ectopic BRG1 expression (Fig. 5E and F). In contrast, knockdown of p53 had no significant effects on SAHF formation induced by ectopic BRG1 expression (Fig. 5E and F). Based on these results, we conclude that knockdown of pRB, $p16^{INK4a}$, or $p21^{CIP1}$, but not p53, inhibits SAHF formation induced by ectopic BRG1 expression.

BRCA1 knockdown induces both SAHF formation and the DNA damage response (14), and suppression of the DNA damage response impairs SAHF formation (37). We next sought to determine the effects of knockdown of pRB, $p16^{INK4a}$, $p21^{CIP1}$, or p53 on SAHF formation induced by BRCA1 knockdown. Notably, knockdown of pRB, $p16^{INK4a}$, $p21^{CIP1}$, or p53 inhibited SAHF formation (Fig. 5G to I). Since knockdown of p53 suppresses SAHF formation induced by knockdown of BRCA1 but not ectopic BRG1 (Fig. 5), these data further support the premise that BRG1 functions downstream of BRCA1 knockdown to drive SAHF formation.

DISCUSSION

The role of BRG1 in SAHF formation induced by BRCA1 knockdown or BRCA1 chromatin dissociation. Here we demonstrated that the interaction between BRG1 and BRCA1 was regulated during RAS-induced senescence (Fig. 1C and D). In addition, chromatin-associated BRG1 levels were increased in cells undergoing senescence induced by oncogenic RAS or BRCA1 knockdown (Fig. 1D and 4K). Consistently, ectopic BRG1 expression drove formation of SAHF and senescence (Fig. 2). Conversely, knockdown of BRG1 inhibited the formation of SAHF induced by oncogenic RAS or BRCA1 knockdown (Fig. 3 and 4). Further, we demonstrated that ectopic BRG1 enhanced SAHF formation induced by BRCA1 knockdown, which resulted in a more pronounced senescence phenotype (Fig. 4). However, BRG1 did not dissociate BRCA1 from chromatin (Fig. 2). Interestingly, BRG1's role in promoting SAHF formation is independent of the DNA damage response (Fig. 2F to H, 3F, and 4D to F; see also Fig. S2 and S4 in the supplemental material), while BRCA1 chromatin dissociation or knockdown induces both SAHF formation and DNA damage response (14). Consistently, knockdown of p53 inhibited SAHF formation induced by BRCA1 knockdown but not by ectopic BRG1 (Fig. 5). Together, these results support the premise that BRG1 acts downstream of BRCA1 to promote SAHF formation during senescence (Fig. 6). In addition, they suggest that oncogene-induced BRCA1 chromatin dissociation contributes to the accumulation of DNA damage observed in senescent cells through BRG1-independent mechanisms (Fig. 6). In agreement with this conclusion, we have previously shown that BRCA1-mediated DNA repair is impaired during RAS-induced senescence (14).

We show that the interaction between BRCA1 and BRG1 is

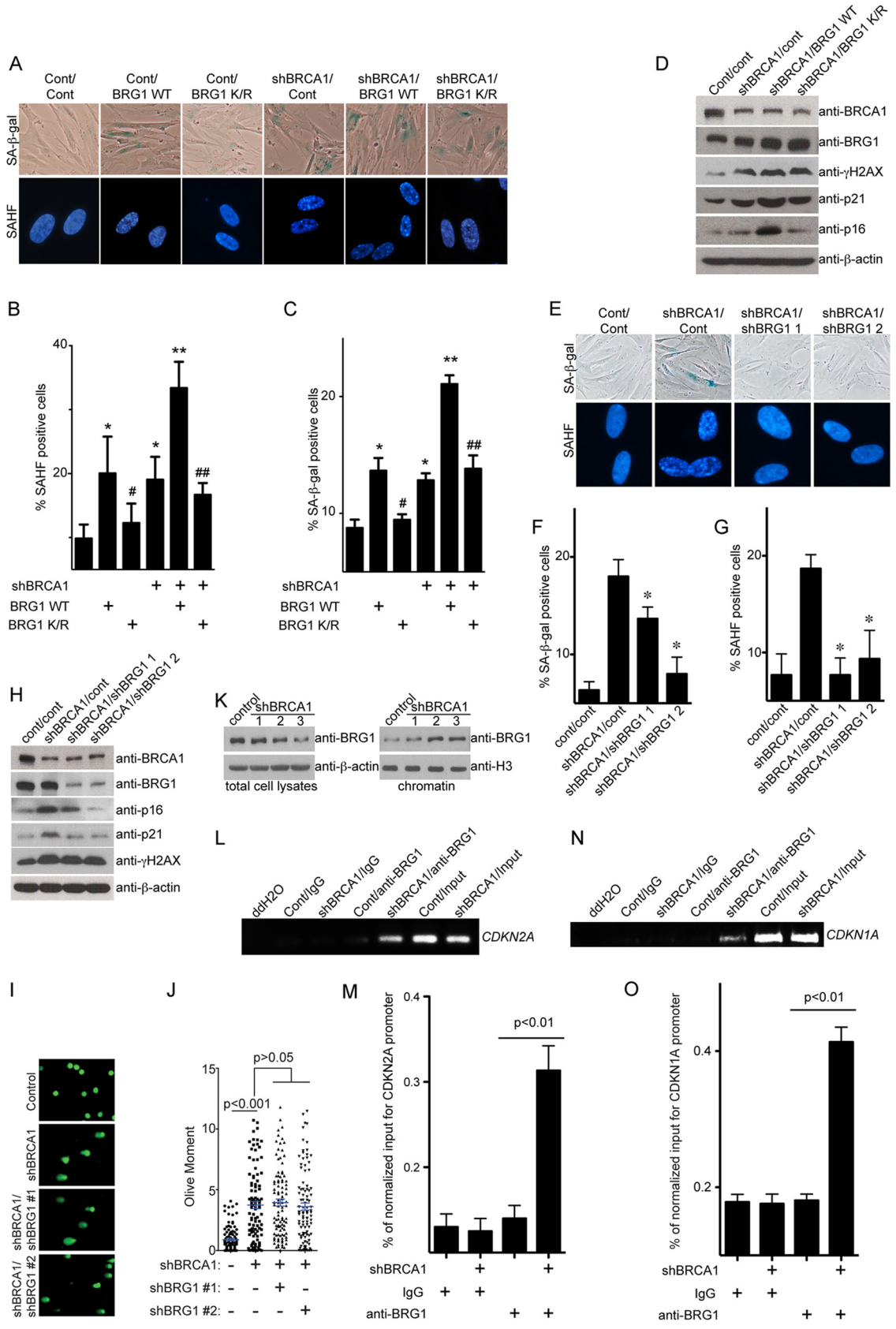

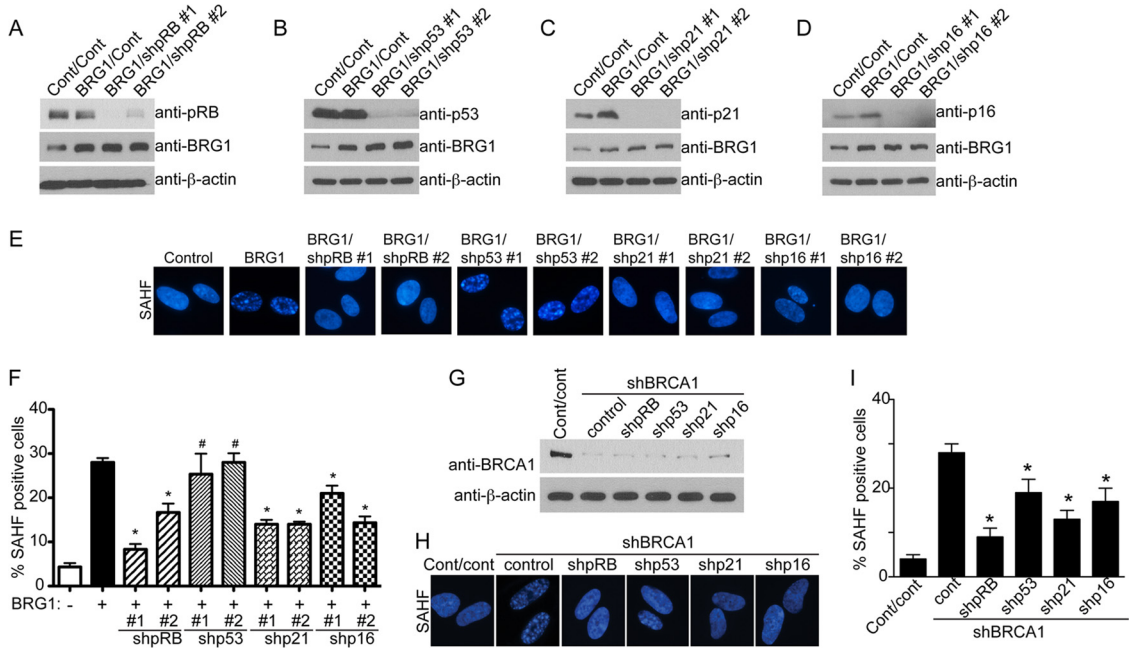

FIG 5 Knockdown of pRB, $p21^{CIP1}$, or $p16^{INK4a}$, but not p53, inhibits SAHF formation induced by ectopic BRG1 expression. (A) IMR90 cells were infected with retrovirus encoding BRG1 together with lentivirus encoding the indicated shpRB or the control. Drug-selected cells were examined for expression of pRB, BRG1, and β-actin by immunoblotting using the indicated antibodies. (B) Same as described for panel A except that cells were examined for expression of shp53. (C) Same as described for panel A except that cells were examined for expression of shp21. (D) Same as described for panel A except that cells were examined for expression of shp16. (E) Same as described for panels A to D except that cells were stained with DAPI to visualize SAHF formation. (F) Quantification of the results shown in panel E. A total of 200 cells from each of the indicated groups were examined for SAHF formation. Data represent the means of the results of three independent experiments with SD. *, $P < 0.05$ (compared with BRG1-expressing cells); #, $P > 0.05$ (compared with BRG1-expressing cells). (G) IMR90 cells were infected with lentivirus encoding shBRCA1 (#3) together with lentivirus encoding the indicated shpRB (#1), shp53 (#2), shp21 (#1), shp16 (#2), or the control. Drug-selected cells were examined for expression of BRCA1 and β-actin by immunoblotting using the indicated antibodies. Please see panel A for the knockdown efficacy of the indicated shRNAs. (H) Same as described for panel G except that cells were stained with DAPI to visualize SAHF formation. (I) Quantification of the results shown in panel H. A total of 200 cells from each of the indicated groups were examined for SAHF formation. Data represent the means of the results of three independent experiments with SD. *, $P < 0.05$ (compared with cells expressing only shBRCA1).

disrupted during senescence, which correlates with the dissociation of BRCA1 from chromatin and an enhanced association of BRG1 with chromatin (Fig. 1). Consistently, the colocalization between BRG1 and BRCA1 was decreased in the nuclei of senescent cells (Fig. 1E). BRCA1 knockdown, which mimics BRCA1 chromatin dissociation and the disruption of the interaction between BRCA1 and BRG1, increased the levels of chromatin-associated BRG1 (Fig. 4K). In contrast, BRG1 overexpression did not affect BRCA1 chromatin association (Fig. 2K). Together, these results suggest that BRCA1 chromatin dissociation and disruption

FIG 4 Knockdown of BRG1 suppresses SAHF formation and senescence induced by BRCA1 knockdown. (A) IMR90 cells were infected with lentivirus encoding shBRCA1 (#3) together with retrovirus encoding wild-type BRG1 (BRG1 WT) or a mutant BRG1 that is defective in chromatin remodeling (BRG1 K/R). Drug-selected cells were stained for SA-β-gal activity or with DAPI to visualize SAHF formation. (B and C) Quantitation of the results shown in panel A. A total of 200 cells from each of the indicated groups were examined for SA-β-gal activity or SAHF formation. Data represent the means of the results of three independent experiments with SD. *, $P < 0.05$ (compared with controls); #, $P > 0.05$ (compared with controls); **, $P < 0.05$ (compared with either shBRCA1 alone or BRG1 WT alone); ##, $P > 0.05$ (compared with shBRCA1 alone). (D) Same as described for panel A but examined for expression of BRCA1, BRG1, γH2AX, $p21^{CIP1}$, and $p16^{INK4a}$ by immunoblotting. Expression of β-actin was used as a loading control. (E) IMR90 cells were infected with retrovirus encoding shBRCA1 (#3) together with indicated shBRG1 or the control. Drug-selected cells were stained for SA-β-gal activity or with DAPI to visualize SAHF formation. (F and G) Quantitation of the results shown in panel E. A total of 200 cells from each of the indicated groups were examined for SA-β-gal activity or SAHF formation. Data represent the means of the results of three independent experiments with SD. *, $P < 0.05$ (compared with shBRCA1-alone cells). (H) Same as described for panel E except that cells were examined for expression of BRCA1, BRG1, γH2AX, $p16^{INK4a}$, and $p21^{CIP1}$ by immunoblotting. Expression of β-actin was used as a loading control. (I) Same as described for panel E except that measurements to determine the extent of DNA damage were performed using the comet assay. (J) Quantification of the results shown in panel I. The extent of DNA damage measured by the comet assay was calculated in artificial Olive Moment units as described in Materials and Methods. Olive Moment levels in 100 cells from each group were measured. Means of the data representing Olive Moment units with standard errors of the means (SEM) are shown in blue. (K) IMR90 cells were infected with lentivirus encoding the indicated shBRCA1 or the control. Drug-selected cells were subjected to fractionation to prepare chromatin, and the expression of BRG1 in the total cell lysates and the chromatin fraction of the indicated cells was examined by immunoblotting. Expression of β-actin and histone H3 was used as a loading control. Please see Fig. 1A for the shBRCA1 knockdown efficacy. (L) IMR90 cells were infected with lentivirus encoding shBRCA1 (#3) or the control. Drug-selected cells were used to perform ChIP analysis using an anti-BRG1 antibody. An isotype-matched IgG was used as a negative control for ChIP analysis. The immunoprecipitated DNA was subjected to PCR analysis using primers that amplify the promoter region of the human *CDKN2A* gene. (M) Same as described for panel L except that the immunoprecipitated DNA was subjected to quantitative PCR analysis. Data represent the means of the results of three independent experiments with SD. (N and O) Same as described for panels L and M except that the human *CDKN1A* gene promoter was analyzed.

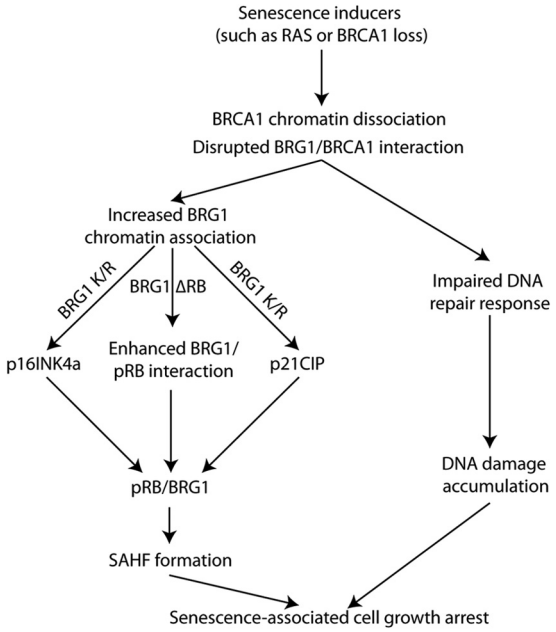

FIG 6 A model for the role of BRG1 in regulating SAHF formation and senescence downstream of BRCA1 loss or oncogenic RAS, which triggers BRCA1 chromatin dissociation.

of the BRCA1 and BRG1 interaction, which act upstream of BRG1 during senescence, are associated (Fig. 6). Our data also show that the interaction between BRCA1 and BRG1 was present in the soluble fractions (Fig. 1C). These data are consistent with a model whereby soluble BRCA1 sequesters BRG1 away from chromatin and disruption of the interaction between BRCA1 and BRG1 causes an enhanced association of BRG1 with chromatin during senescence.

Molecular mechanisms by which BRG1 promote SAHF formation. BRG1 is known to regulate heterochromatin structure. Indeed, BRG1 interacts with pRB, which is known to play a key role in regulating SAHF formation (7, 22). Here we show that the interaction between BRG1 and pRB was enhanced during senescence and that formation of SAHF induced by ectopic BRG1 required its interaction with pRB (Fig. 1F and 2L to N). Consistently, knockdown of pRB suppressed SAHF formation induced by ectopic BRG1 expression (Fig. 5). However, the BRG1 ΔRB mutant did not affect upregulation of $p16^{INK4a}$ and $p21^{CIP1}$ (Fig. 2O). In contrast, a chromatin-remodeling-activity-deficient BRG1 mutant (BRG1 K798R) that failed to induce $p16^{INK4a}$ and $p21^{CIP1}$ expression was unable to drive SAHF formation (Fig. 2B and C). These data suggest that the BRG1 and pRB complex acts downstream of $p16^{INK4a}$ and $p21^{CIP1}$, whose expression requires BRG1's chromatin-remodeling activity (Fig. 6). Indeed, both $p16^{INK4a}$ and $p21^{CIP1}$ are known regulators of pRB (38). Together, these data support the notion that the complex of BRG1 and pRB functions downstream of $p16^{INK4a}$ and $p21^{CIP1}$ to promote SAHF formation (Fig. 6).

It has been demonstrated that $p16^{INK4a}$ and pRB are necessary for SAHF formation during senescence induced by oncogenic RAS (7). However, p53 and $p21^{CIP1}$ are not necessary for SAHF formation in this context (7). In contrast, both p53 and $p21^{CIP1}$ are required for SAHF formation induced by knockdown of adenovirus E1A-associated p400 protein (9). Here we show that ectopic BRG1 induced the expression of $p21^{CIP1}$ and $p16^{INK4a}$ but had no effects on p53 expression (Fig. 2F). This is consistent with a previous report showing that BRG1-induced upregulation of $p21^{CIP1}$ is independent of p53 (24). Notably, the association of BRG1 with the promoters of the *CDKN2A* and *CDKN1A* genes, which encode pRB regulators $p16^{INK4a}$ and $p21^{CIP1}$, was enhanced during senescence induced by oncogenic RAS or BRCA1 knockdown (Fig. 3G to J and 4L to O). In addition, we demonstrated that knockdown of BRG1 suppressed SAHF formation, which correlates with suppression of expression of both $p16^{INK4a}$ and $p21^{CIP1}$ induced by BRCA1 knockdown or oncogenic RAS (Fig. 3 and 4). Further, knockdown of $p16^{INK4a}$, $p21^{CIP1}$, or pRB, but not p53, inhibited SAHF formation induced by ectopic BRG1 expression (Fig. 5). Together, these data support a model whereby BRG1 promotes SAHF formation via its interaction with pRB, which is regulated by the upregulation of $p16^{INK4a}$ and $p21^{CIP1}$ through its chromatin-remodeling activity (Fig. 6).

BRG1, DNA damage, and SAHF. Here we showed that ectopic BRG1 drives SAHF formation and that this is independent of the DNA damage response by multiple markers (Fig. 2F to H; see also Fig. S2 in the supplemental material). These DNA damage markers include expression of γH2AX, p53, and serine 15-phosphorylated p53 (Fig. 2F). Consistently, BRG1 did not affect the extent of DNA damage in these cells, as measured by the comet assay (Fig. 2G and H). Conversely, knockdown of BRG1 inhibited SAHF formation induced by oncogenic RAS or BRCA1 knockdown with no overt effects on the DNA damage response (Fig. 3F and 4H to J; see also Fig. S4 in the supplemental material). Interestingly, previous evidence suggests that formation of SAHF limits the extent of DNA damage induced by oncogenic RAS (37). Likewise, it has been demonstrated that ectopic $p16^{INK4a}$ drives SAHF formation. However, $p16^{INK4a}$-induced senescence displays little DNA damage response (39). Together, our data suggest that DNA damage is not necessary for SAHF formation.

In summary, we showed that the interaction between BRG1 and BRCA1 is regulated during senescence. BRG1 is required for SAHF formation and senescence induced by BRCA1 knockdown or oncogenic RAS, which triggers BRCA1 chromatin dissociation. This correlates with an increase in chromatin-associated BRG1 levels. The association of BRG1 with the promoters of *CDKN2A* and *CDKN1A* genes is enhanced during senescence and correlates with the upregulation of $p16^{INK4a}$ and $p21^{CIP1}$ in a chromatin-remodeling-activity-dependent manner. In addition, the interaction between BRG1 and pRB is enhanced during senescence and SAHF formation induced by ectopic BRG1 requires its interaction with pRB. Further, $p16^{INK4a}$ and $p21^{CIP1}$ act upstream of pRB to mediate SAHF formation induced by ectopic BRG1 (Fig. 6). Thus, our current report sheds new light on how BRG1 regulates SAHF formation and senescence downstream of BRCA1 loss or oncogenic RAS that triggers BRCA1 chromatin dissociation.

ACKNOWLEDGMENTS

We thank Katherine Aird, Benjamin Bitler, and Michael Amatangelo for critical reading of the manuscript and other members of the laboratory for discussions and suggestions.

This work was supported by a NIH/NCI grant (R01CA160331 to R.Z.) and, in part, by a DOD award (OC093420 to R.Z.). Support of core facilities used in this study was provided by Cancer Center Support Grant CA010815 to The Wistar Institute.

REFERENCES

1. **Campisi J.** 2005. Senescent cells, tumor suppression, and organismal aging: good citizens, bad neighbors. Cell **120**:513–522.
2. **Adams PD.** 2009. Healing and hurting: molecular mechanisms, functions, and pathologies of cellular senescence. Mol. Cell **36**:2–14.
3. **Dimri GP, Lee X, Basile G, Acosta M, Scott G, Roskelley C, Medrano EE, Linskens M, Rubelj I, Pereira-Smith O, Peacocke M, Campisi J.** 1995. A biomarker that identifies senescent human cells in culture and in aging skin in vivo. Proc. Natl. Acad. Sci. U. S. A. **92**:9363–9367.
4. **Zhang R, Chen W, Adams PD.** 2007. Molecular dissection of formation of senescence-associated heterochromatin foci. Mol. Cell. Biol. **27**:2343–2358.
5. **Zhang R, Poustovoitov MV, Ye X, Santos HA, Chen W, Daganzo SM, Erzberger JP, Serebriiskii IG, Canutescu AA, Dunbrack RL, Pehrson JR, Berger JM, Kaufman PD, Adams PD.** 2005. Formation of MacroH2A-containing senescence-associated heterochromatin foci and senescence driven by ASF1a and HIRA. Dev. Cell **8**:19–30.
6. **Narita M, Krizhanovsky V, Nunez S, Chicas A, Hearn SA, Myers MP, Lowe SW.** 2006. A novel role for high-mobility group a proteins in cellular senescence and heterochromatin formation. Cell **126**:503–514.
7. **Narita M, Nunez S, Heard E, Lin AW, Hearn SA, Spector DL, Hannon GJ, Lowe SW.** 2003. Rb-mediated heterochromatin formation and silencing of E2F target genes during cellular senescence. Cell **113**:703–716.
8. **Braig M, Lee S, Loddenkemper C, Rudolph C, Peters AH, Schlegelberger B, Stein H, Dorken B, Jenuwein T, Schmitt CA.** 2005. Oncogene-induced senescence as an initial barrier in lymphoma development. Nature **436**:660–665.
9. **Chan HM, Narita M, Lowe SW, Livingston DM.** 2005. The p400 E1A-associated protein is a novel component of the p53 → p21 senescence pathway. Genes Dev. **19**:196–201.
10. **Di Micco R, Fumagalli M, Cicalese A, Piccinin S, Gasparini P, Luise C, Schurra C, Garre M, Nuciforo PG, Bensimon A, Maestro R, Pelicci PG, d'Adda di Fagagna F.** 2006. Oncogene-induced senescence is a DNA damage response triggered by DNA hyper-replication. Nature **444**:638–642.
11. **Bartkova J, Rezaei N, Liontos M, Karakaidos P, Kletsas D, Issaeva N, Vassiliou LV, Kolettas E, Niforou K, Zoumpourlis VC, Takaoka M, Nakagawa H, Tort F, Fugger K, Johansson F, Sehested M, Andersen CL, Dyrskjot L, Orntoft T, Lukas J, Kittas C, Helleday T, Halazonetis TD, Bartek J, Gorgoulis VG.** 2006. Oncogene-induced senescence is part of the tumorigenesis barrier imposed by DNA damage checkpoints. Nature **444**:633–637.
12. **Scully R, Livingston DM.** 2000. In search of the tumour-suppressor functions of BRCA1 and BRCA2. Nature **408**:429–432.
13. **Gudmundsdottir K, Ashworth A.** 2006. The roles of BRCA1 and BRCA2 and associated proteins in the maintenance of genomic stability. Oncogene **25**:5864–5874.
14. **Tu Z, Aird KM, Bitler BG, Nicodemus JP, Beeharry N, Zia B, Yen TJ, Zhang R.** 2011. Oncogenic Ras regulates BRIP1 expression to induce dissociation of BRCA1 from chromatin, inhibit DNA repair, and promote senescence. Dev. Cell **21**:1077–1091.
15. **Cao L, Li W, Kim S, Brodie SG, Deng CX.** 2003. Senescence, aging, and malignant transformation mediated by p53 in mice lacking the Brca1 full-length isoform. Genes Dev. **17**:201–213.
16. **Cao L, Kim S, Xiao C, Wang RH, Coumoul X, Wang X, Li WM, Xu XL, De Soto JA, Takai H, Mai S, Elledge SJ, Motoyama N, Deng CX.** 2006. ATM-Chk2-p53 activation prevents tumorigenesis at an expense of organ homeostasis upon Brca1 deficiency. EMBO J. **25**:2167–2177.
17. **Ye Q, Hu YF, Zhong H, Nye AC, Belmont AS, Li R.** 2001. BRCA1-induced large-scale chromatin unfolding and allele-specific effects of cancer-predisposing mutations. J. Cell Biol. **155**:911–921.
18. **Bochar DA, Wang L, Beniya H, Kinev A, Xue Y, Lane WS, Wang W, Kashanchi F, Shiekhattar R.** 2000. BRCA1 is associated with a human SWI/SNF-related complex: linking chromatin remodeling to breast cancer. Cell **102**:257–265.
19. **Reisman D, Glaros S, Thompson EA.** 2009. The SWI/SNF complex and cancer. Oncogene **28**:1653–1668.
20. **Bultman S, Gebuhr T, Yee D, La Mantia C, Nicholson J, Gilliam A, Randazzo F, Metzger D, Chambon P, Crabtree G, Magnuson T.** 2000. A Brg1 null mutation in the mouse reveals functional differences among mammalian SWI/SNF complexes. Mol. Cell **6**:1287–1295.
21. **Bultman SJ, Herschkowitz JI, Godfrey V, Gebuhr TC, Yaniv M, Perou CM, Magnuson T.** 2008. Characterization of mammary tumors from Brg1 heterozygous mice. Oncogene **27**:460–468.
22. **Dunaief JL, Strober BE, Guha S, Khavari PA, Alin K, Luban J, Begemann M, Crabtree GR, Goff SP.** 1994. The retinoblastoma protein and BRG1 form a complex and cooperate to induce cell cycle arrest. Cell **79**:119–130.
23. **Ye X, Zerlanko B, Zhang R, Somaiah N, Lipinski M, Salomoni P, Adams PD.** 2007. Definition of pRB- and p53-dependent and -independent steps in HIRA/ASF1a-mediated formation of senescence-associated heterochromatin foci. Mol. Cell. Biol. **27**:2452–2465.
24. **Hendricks KB, Shanahan F, Lees E.** 2004. Role for BRG1 in cell cycle control and tumor suppression. Mol. Cell. Biol. **24**:362–376.
25. **Trouche D, Le Chalony C, Muchardt C, Yaniv M, Kouzarides T.** 1997. RB and hbrm cooperate to repress the activation functions of E2F1. Proc. Natl. Acad. Sci. U. S. A. **94**:11268–11273.
26. **Napolitano MA, Cipollaro M, Cascino A, Melone MA, Giordano A, Galderisi U.** 2007. Brg1 chromatin remodeling factor is involved in cell growth arrest, apoptosis and senescence of rat mesenchymal stem cells. J. Cell Sci. **120**:2904–2911.
27. **Naidu SR, Love IM, Imbalzano AN, Grossman SR, Androphy EJ.** 2009. The SWI/SNF chromatin remodeling subunit BRG1 is a critical regulator of p53 necessary for proliferation of malignant cells. Oncogene **28**:2492–2501.
28. **Zhang R, Liu ST, Chen W, Bonner M, Pehrson J, Yen TJ, Adams PD.** 2007. HP1 proteins are essential for a dynamic nuclear response that rescues the function of perturbed heterochromatin in primary human cells. Mol. Cell. Biol. **27**:949–962.
29. **Ye X, Zerlanko B, Kennedy A, Banumathy G, Zhang R, Adams PD.** 2007. Downregulation of Wnt signaling is a trigger for formation of facultative heterochromatin and onset of cell senescence in primary human cells. Mol. Cell **27**:183–196.
30. **Li H, Cai Q, Godwin AK, Zhang R.** 2010. Enhancer of zeste homolog 2 promotes the proliferation and invasion of epithelial ovarian cancer cells. Mol. Cancer Res. **8**:1610–1618.
31. **Méndez J, Stillman B.** 2000. Chromatin association of human origin recognition complex, cdc6, and minichromosome maintenance proteins during the cell cycle: assembly of prereplication complexes in late mitosis. Mol. Cell. Biol. **20**:8602–8612.
32. **Kia SK, Gorski MM, Giannakopoulos S, Verrijzer CP.** 2008. SWI/SNF mediates polycomb eviction and epigenetic reprogramming of the INK4b-ARF-INK4a locus. Mol. Cell. Biol. **28**:3457–3464.
33. **Bourgo RJ, Siddiqui H, Fox S, Solomon D, Sansam CG, Yaniv M, Muchardt C, Metzger D, Chambon P, Roberts CW, Knudsen ES.** 2009. SWI/SNF deficiency results in aberrant chromatin organization, mitotic failure, and diminished proliferative capacity. Mol. Biol. Cell **20**:3192–3199.
34. **Sif S, Saurin AJ, Imbalzano AN, Kingston RE.** 2001. Purification and characterization of mSin3A-containing Brg1 and hBrm chromatin remodeling complexes. Genes Dev. **15**:603–618.
35. **Strober BE, Dunaief JL, Guha S, Goff SP.** 1996. Functional interactions between the hBRM/hBRG1 transcriptional activators and the pRB family of proteins. Mol. Cell. Biol. **16**:1576–1583.
36. **Kang H, Cui K, Zhao K.** 2004. BRG1 controls the activity of the retinoblastoma protein via regulation of p21CIP1/WAF1/SDI. Mol. Cell. Biol. **24**:1188–1199.
37. **Di Micco R, Sulli G, Dobreva M, Liontos M, Botrugno OA, Gargiulo G, Dal Zuffo R, Matti V, d'Ario G, Montani E, Mercurio C, Hahn WC, Gorgoulis V, Minucci S, d'Adda di Fagagna F.** 2011. Interplay between oncogene-induced DNA damage response and heterochromatin in senescence and cancer. Nat. Cell Biol. **13**:292–302.
38. **Ortega S, Malumbres M, Barbacid M.** 2002. Cyclin D-dependent kinases, INK4 inhibitors and cancer. Biochim. Biophys. Acta **1602**:73–87.
39. **Rodier F, Coppe JP, Patil CK, Hoeijmakers WA, Munoz DP, Raza SR, Freund A, Campeau E, Davalos AR, Campisi J.** 2009. Persistent DNA damage signalling triggers senescence-associated inflammatory cytokine secretion. Nat. Cell Biol. **11**:973–979.

Supplemental Figures and Figure Legends

Tu et al, Supplementary Figure 1

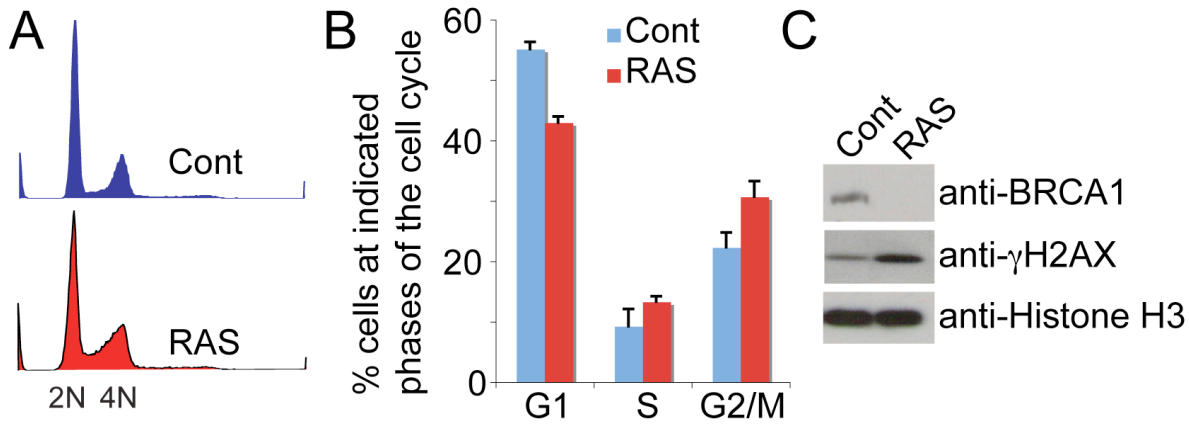

Figure S1. BRCA1 chromatin dissociation is not a consequence of G1 phase accumulation during oncogene-induced senescence.

(A) IMR90 cells were infected with control (C) or RAS (R) -encoding retrovirus. Two days post-infection, the infected cells were examined for cell cycle distribution by flow cytometry.

(B) Quantitation of (A). Mean of three independent experiments with SD.

(C) Same as (A) but the cells were subjected to fractionation to prepare chromatin and the expression of BRCA1 and γH2AX in the chromatin fraction of the indicated cells was examined by immunoblotting. Expression of core histone H3 was used as a loading control.

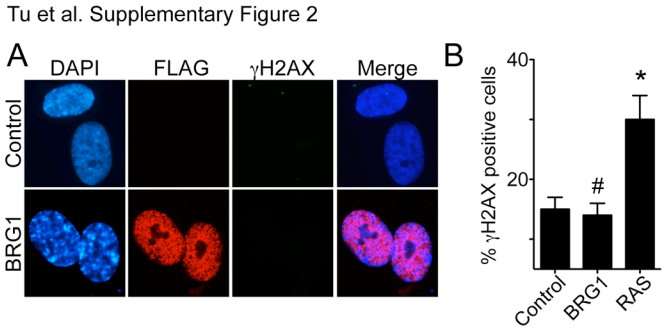

Figure S2. Ectopic BRG1 expression does not increase γH2AX foci formation.

(A) IMR90 cells were infected with retrovirus encoding FLAG tagged wild type BRG1 or control. Infected cells were stained with an anti-FLAG antibody and an anti-γH2AX antibody.

(B) 200 cells from FLAG positively stained FLAG-BRG1 infected cells or controls were examined for γH2AX foci formation. RAS-infected cells were used as a positive controls. Mean of three independent experiments with SD. # $p>0.05$ and * $p<0.05$ vs. controls.

Tu et al. Supplementary Figure 3

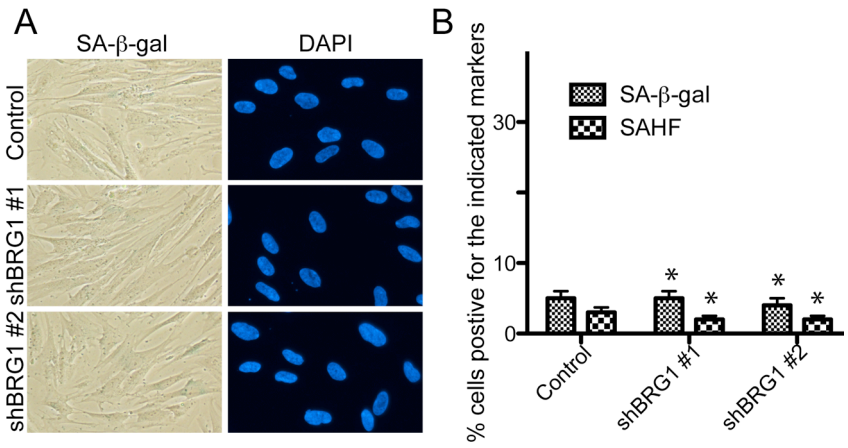

Figure S3. BRG1 knockdown alone does not induce senescence.

(A) IMR90 cells were infected with lentivirus encoding the indicated shBRG1 or control. Drug-selected cells were stained for SA-b-gal activity or with DAPI to visualize SAHF. (B) Quantification of (A). Mean of three independent experiments with SD. * p>0.05 compared with controls.

Tu et al. Supplementary Figure 4

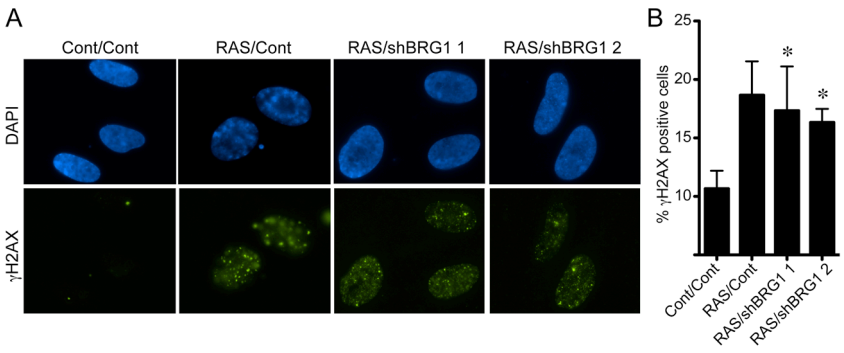

Figure S4. BRG1 knockdown does not suppress the DNA damage response induced by oncogenic RAS.

(A) IMR90 cells were infected with retrovirus encoding oncogenic H-RAS^{G12V} or control together with lentivirus encoding the indicated shBRG1 or control. Formation of γH2AX foci was visualized by staining the cells with an anti-γH2AX antibody.

(B) Quantitation of (A). 200 cells from each of the indicated groups were examined for γH2AX foci formation. Mean of three independent experiments with SD. * p>0.05 compared with RAS alone cells.

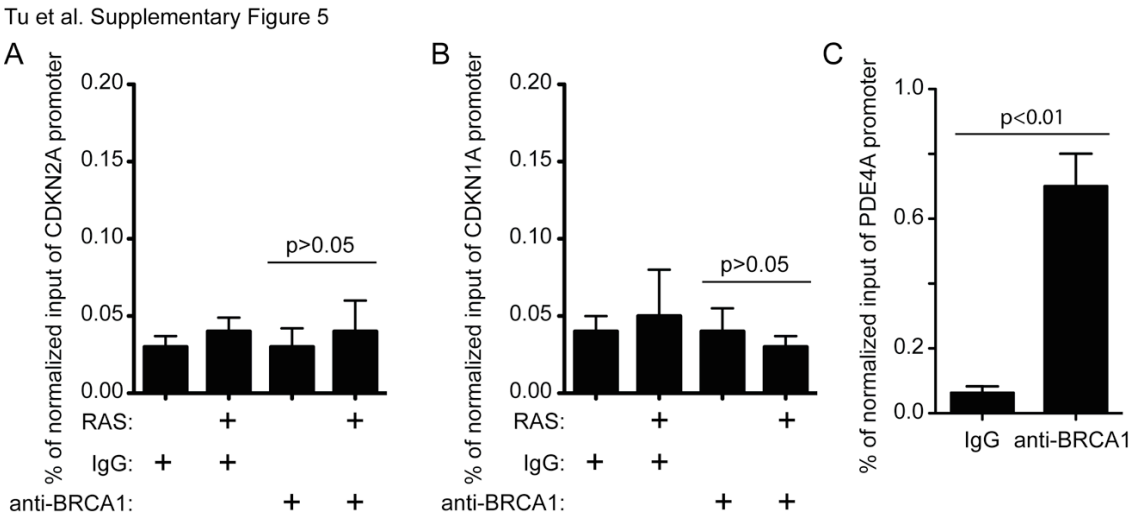

Figure S5. The association of BRCA1 with the promoter of the human *CDKN2A* and *CDKN1A* genes is not significantly affected during oncogene-induced senescence.

(A) IMR90 cells were infected with retrovirus encoding H-RAS^{G12V} or control. Drug-selected cells were used to perform ChIP analysis using an anti-BRCA1 antibody. An isotype matched IgG was used as a negative control for ChIP analysis. The immunoprecipitated DNA was subjected to PCR analysis using primers that amplify the promoter region of the human *CDKN2A* gene.

(B) Same as (A) but for the human *CDKN1A* gene promoter.

(C) Same as (A) but for the human *PDE4A* gene promoter, a known BRCA1 target gene (1).

1. **Gorski JJ, Savage KI, Mulligan JM, McDade SS, Blayney JK, Ge Z, Harkin DP.** 2011. Profiling of the BRCA1 transcriptome through microarray and ChIP-chip analysis. Nucleic acids research **39:**9536-9548.